Letter | Editors' Suggestion

Cavity optomechanics with a laser-engineered optical trap

P. Sesin,[1] S. Anguiano,[1] A. E. Bruchhausen,[1] A. Lemaître,[2] and A. Fainstein[1,*]

[1]*Centro Atómico Bariloche and Instituto Balseiro, CNEA, and CONICET, Universidad Nacional de Cuyo, Avenida E. Bustillo 9500, R8402AGP San Carlos de Bariloche, Río Negro, Argentina*

[2]*Centre de Nanosciences et de Nanotechnologies, CNRS, Université Paris-Sud, Université Paris-Saclay, 10 Boulevard Thomas Gobert, 91120 Palaiseau, France*

(Received 13 October 2020; revised 29 December 2020; accepted 25 January 2021; published 10 February 2021)

Laser-engineered exciton-polariton networks could lead to dynamically configurable integrated optical circuitry and quantum devices. Combining cavity optomechanics with electrodynamics in laser-configurable hybrid designs constitutes a platform for the vibrational control, conversion, and transport of signals. With this aim we investigate three-dimensional optical traps laser induced in quantum well embedded semiconductor planar microcavities. We show that the laser-generated and -controlled discrete states of the traps dramatically modify the interaction between photons and phonons confined in the resonators, accessing through coupling of photoelastic origin ($g_0/2\pi \sim 1.8$ MHz) an optomechanical cooperativity $C > 1$ for milliwatt excitation. The quenching of Stokes processes and double-resonant enhancement of anti-Stokes ones involving pairs of discrete optical states in the sideband-resolved regime allow the optomechanical cooling of 180-GHz bulk acoustic waves, starting from room temperature down to ∼130 K. These results pave the way for dynamical tailoring of optomechanical actuation in the extremely high frequency range (30–300 GHz) for future network and quantum technologies.

DOI: 10.1103/PhysRevB.103.L081301

Introduction. Trapping and potential landscape engineering through nonresonant laser excitation is used in the exciton-polariton domain to modify the polaritons spatial distribution, their spectra, and dynamics, including the formation of one- and two-dimensional lattices, with prospects for new devices and quantum simulators [1–9]. In these experiments the applied laser defines an effective potential for the exciton polaritons, actuating on either their excitonic or photonic component. The physical mechanism that acts on the excitonic component is the Coulomb repulsion, which increases the energy of the coupled particles [2–6]. The action on the photonic component depends on local laser-induced variations of the refractive index, usually defining attractive potentials [7,8]. This latter strategy can also be used to generate confining cavities, or more arbitrary effective potentials, for pure photons [7].

Lasers are routinely used in atomic physics to engineer optical traps for atoms and, in addition, to laser cool them by quenching the atom motion through so-called Doppler cooling [10–13]. Laser trapping by optical tweezers with vibrational cooling or stimulation was also demonstrated recently for center-of-mass oscillations of nanoparticles levitated in vacuum [14–16]. Concepts related to Doppler cooling are also applied in a variety of solid systems for optomechanical dynamical back-action phenomena [17–19], including cooling of mechanical vibrations (even down to the quantum limit) [20–24] and laser-induced mechanical self-oscillation [25,26]. To the best of our knowledge, however, such cavity optomechanical phenomena have not been reported in condensed-matter laser-engineered optical resonators.

In this work we demonstrate optically generated photonic traps as optomechanical devices. A planar semiconductor microcavity with a spacer constituted by a superlattice (SL) with 41 GaAs/AlAs bilayers is shown to one-dimensionally confine photons and vibrations with frequencies as high as ∼180 GHz. Application of a green focused laser beam induces in-plane trapping of photons with full discretization of the optical spectra, strongly enhancing the light-vibrational coupling. We demonstrate single- and double-resonant Brillouin processes and optomechanical cooling of the ∼180-GHz slow phonons of the semiconductor SL from room temperature down to ∼130 K. The laser-induced trap could be dynamically modified so that vibrations are selectively laser cooled or made to self-oscillate, opening the path for a variety of quantum information reconfigurable applications.

Optomechanics with a laser-induced optical trap. The concept of the proposed cavity optomechanical experiments with laser-trapped light is illustrated in Fig. 1. The setup is schematized in Fig. 1(a) and described in the Supplemental Material (SM) [27]. A microscope overlaps three lasers on $\sim 3 - \mu$m spots. The 514.5-nm green line of an Ar-Kr laser ["trap laser" (TL)] is focused to generate a Gaussian-shaped three-dimensional optical trap [7]. A "photoluminescence laser" (PLL) is used with very low power (typically, several microwatts) above the SL exciton gap to characterize through the emission the optical modes of the three-dimensional (3D) cavity. Finally, a third laser tuned to the TL-generated 3D optical trap modes is used to resonantly excite the SL vibrational modes ["Brillouin laser" (BL)]. Figures 1(b)–1(d)

*Corresponding author: afains@cab.cnea.gov.ar

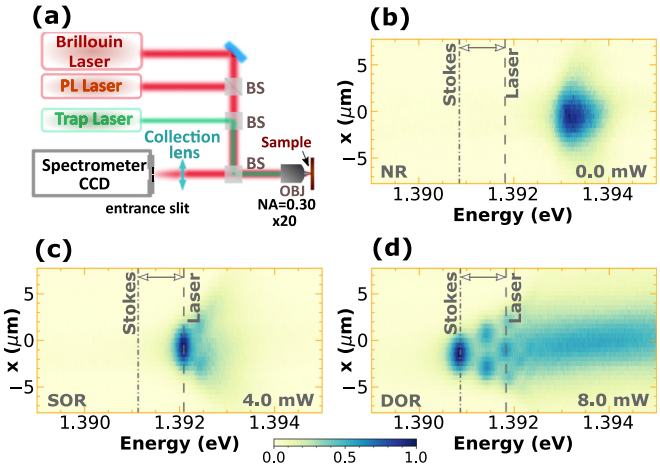

FIG. 1. Cavity optomechanics with laser-generated optical traps. (a) Scheme of the three-laser experimental setup. (b)–(d) Spatial images of the optical cavity modes that evolve with increasing TL power (indicated in each panel) from planar 1D confinement in (b) to fully 3D confined in (c) and (d). The energy of the Brillouin laser and Stokes scattered photons are indicated with vertical lines. In (b) the optomechanical process is nonresonant (NR). The situations corresponding to single (SOR) and double (DOR) optical resonances are attained in (c) and (d), respectively.

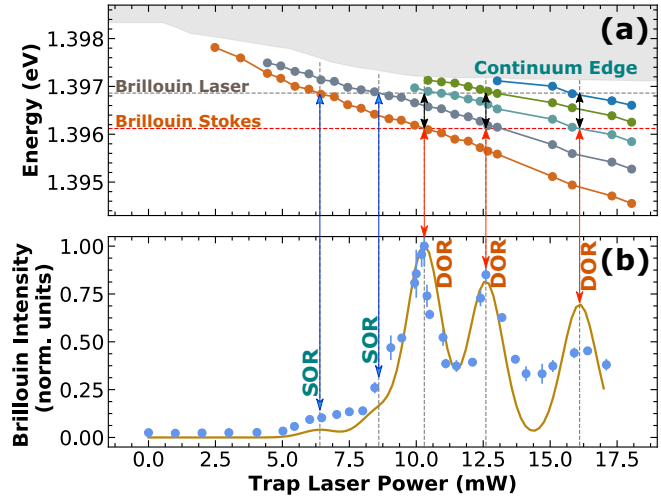

FIG. 2. Optomechanical coupling as a function of trap laser power. (a) Fan plot of the energy of the optical trap modes as a function of TL power. The confined states and the lower edge of the continuum are shown with connected symbols and with a gray background, respectively. Horizontal lines identify the energy of the BL and Stokes scattered photons. Double-pointed black arrows highlight the situations where DOR is attained. (b) Symbols show the Brillouin intensity of the SL slow mode as a function of TL power. Single and double optical resonances are indicated with blue and red vertical arrows, respectively. The curve corresponds to the model discussed in the text. Error bars represent the added experimental and data processing uncertainty. When not shown they are smaller than the symbol size.

show spectrally resolved spatial PL images corresponding to increasing TL power (0, 4, and 8 mW, respectively), obtained with the PLL on and the BL off. The energy of the BL is indicated in the three panels with vertical dashed lines, together with that of the Stokes (redshifted) photons corresponding to the scattering by the ∼180-GHz (∼5.7 cm^{-1}) slow bulk acoustic mode of the GaAs/AlAs SL embedded in the resonator [28,29]. This mode is located at the lower edge of the Brillouin zone center first phononic band gap of the SL and thus has almost zero group velocity. Its slow speed leads to an effective mechanical quality factor $Q_m \sim 10^3$ (see a detailed discussion in the SM [27]). In Fig. 1(b) the broad emission corresponding to the planar microcavity can be observed starting at ∼1.3932 eV and expanding towards higher energies [due to the parabolic dispersion of the one-dimensional (1D) confined optical cavity modes]. This condition corresponds to nonresonant inelastic scattering: neither the BL nor the Stokes photons are resonant with any optical cavity mode. As the TL power is increased to 4 mW [Fig. 1(c)], clear modes of a 3D optical trap emerge, with the fundamental mode having redshifted with respect to the continuum and falling precisely at the energy of the BL. This situation corresponds to an incoming "single optical resonance" (SOR): the BL is resonant, but the Stokes photons are not. Finally, with the TL power at 8 mW [Fig. 1(d)], multiple discrete 3D optical trap modes are evidenced. The fundamental mode has further redshifted to be resonant with the Stokes photons, while the BL is resonant with the third optically confined mode. This situation corresponds to a "double optical resonance" (DOR). For this experiment the separation between the discrete optically confined modes was tuned by choosing the size of the TL illuminated spot, which defines the lateral width of the Gaussian optical confining potential.

Single- and double-resonant cavity optomechanics. Figure 2(a) presents a fan plot with the energies of the 3D trap optical modes as a function of TL power. The energy of the BL and the Stokes photons scattered by the slow vibrational mode of the SL are indicated. Figure 2(b) shows with solid symbols the Brillouin intensity as a function of TL power, associated with the vibrational slow mode (the PL and Brillouin spectra are provided in the SM [27]). Starting from low TL powers, the first two blue vertical arrows highlight situations in which incoming SOR is attained. The BL is resonant with a cavity mode (either the first or second confined mode), but the inelastically scattered Stokes photons are not. Note that we are in the sideband-resolved regime [12,19,24], that is, the frequency of the vibrational modes is larger than the width of the optical cavity modes (the vibrational mode oscillates several periods before the trapped photon escapes from the resonator). This condition is critical for diverse cavity optomechanical phenomena and particularly to attain efficient cooling. One consequence of this sideband-resolved condition is that the SOR Brillouin signals in Fig. 2 are very weak: with no available mode at lower energies the scattered photons cannot escape the resonator, and thus the Stokes process is strongly inhibited.

On increasing the TL power in Fig. 2(b) the Brillouin signal strongly increases, displaying three clear maxima. By correlating these maxima with the fan plot in Fig. 2(a), it follows that the system successively goes through three DORs (indicated by red vertical arrows). These DORs involve first the excitation with the BL through the third optical trap

state and scattering through the first ($3 \rightarrow 1$), with increasing power successively $4 \rightarrow 2$ and $5 \rightarrow 3$. The magnitude of this trap-enhanced optomechanical coupling decreases as the order of the involved optical modes increases. As we will argue below, the optomechanical coupling scales as $1/D$, where D is the lateral diameter of the involved trap-confined mode [30]. Because of the Gaussian shape of the laser-induced optical trap [7], modes are laterally less confined as their order increases. The accessed DORs could allow for optomechanical cooling and stimulation, which will be addressed next.

Optomechanical cooling. The relevant consequences of dynamical back-action in cavity optomechanics are the possibilities to cool, or, alternatively, stimulate, the mechanical motion by *cw* laser excitation [17–19]. The standard way to cool (stimulate) a mechanical mode with a single optical mode is by red-detuned (blue-detuned) laser excitation of the latter. This process is most efficient when the detuning between the laser and the involved optical cavity mode equals the energy of the vibrational mode. This method is strongly weakened in the sideband-resolved regime because the transmission of the pump photons into the resonator is strongly reduced (as with the Stokes photons in the SOR discussed above). This problem can be overcome by using two optical cavity modes coupled by the mechanical motion [26,31,32], as we have shown by the DOR with the laser-generated discrete optical states in Fig. 2(b).

We use a two-mode scheme as depicted in Figs. 3(a) and 3(b). The TL power is set at the condition of the strongest DOR shown in Fig. 2(b) ($P_{\mathrm{TL}} \sim 10\,\mathrm{mW}$). Without changing the BL energy, the system is modified to operate in cooling (anti-Stokes) or stimulation (Stokes) conditions simply by displacing the spot on the structure and thus rigidly shifting the optical cavity modes (the planar microcavity is grown with a taper to allow for this tuning). For the two situations the same two optical trap modes participate but interchange their roles. Moreover, the detuning between the BL and the SL exciton resonance is constant, so that for the two processes the laser exciton-mediated photoelastic resonance and eventual residual heating are the same [33]. Thus, the difference between the intensities of the Stokes and anti-Stokes processes is the intervening boson factor, which is proportional to $n+1$ for the creation (Stokes) and n for the destruction (anti-Stokes) of a phonon, with n being the phonon occupation. Consequently, the Stokes and anti-Stokes intensities can be used to obtain n and thus probe the presence of either vibrational pumping or cooling [34–36].

Figure 3(c) presents the BL power dependence of the Stokes (red) and anti-Stokes (blue) signal intensities. A linear dependence with BL power is expected in spontaneous Brillouin scattering (indicated by a dashed straight line extrapolated from the region of low power). Departures from this linear dependence are a signature of higher-order processes (that is, n is not determined by thermal equilibrium but becomes dependent on the BL power). The Stokes contribution follows a linear dependence quite closely, with a possible weak supralinear behavior above ~3 mW. The anti-Stokes signal clearly departs from linearity around ~2.5 mW, displaying a systematic sublinear behavior. From this departure and the fact that at low BL powers the system is in thermal equilibrium (linear region), we can extract the phonon population as a function of BL power for the anti-Stokes configuration, or, equivalently, the effective temperature of the mode [see Fig. 3(d)]. A significant mode cooling from room temperature down to ~130 K is demonstrated, reaching a mode occupation of only ~15 without cryogenic refrigeration. We note that the anti-Stokes scheme depicted in Fig. 3(b) is ideal for optomechanical cooling due to the existent DOR mediated by 3D optical trap modes, and because no modes are available at energies lower than that of the BL.

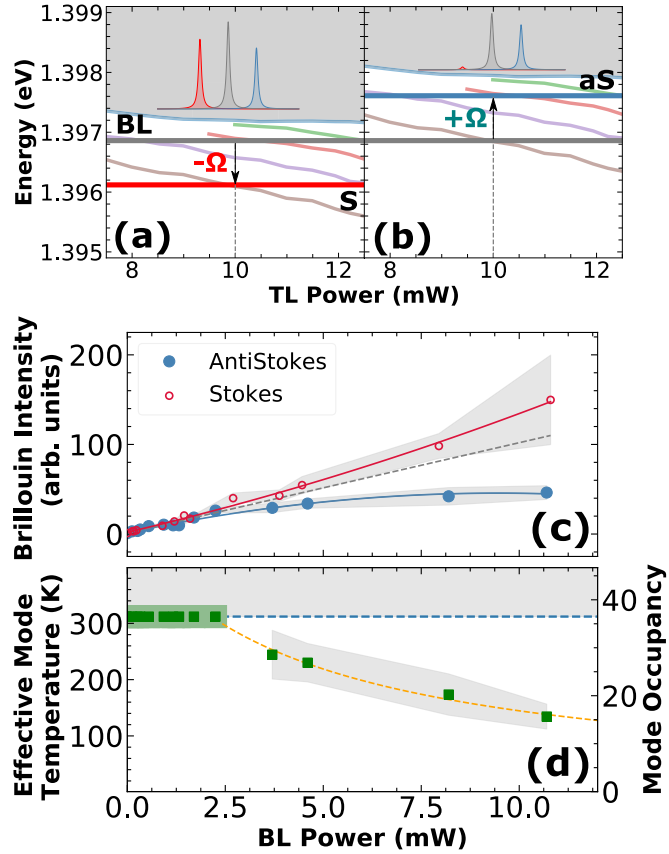

FIG. 3. Optomechanical cooling with a laser-induced optical trap. (a) Schemes of the Stokes (stimulation) and (b) anti-Stokes (cooling) geometries. The colored curves are fan plots describing the optical trap modes as in Fig. 2(a). The energy of the BL and the Stokes (S) and anti-Stokes (aS) photons are indicated with horizontal lines. $\pm\Omega$ correspond to the energy of the SL slow vibration. Note that in (a) both the Stokes and anti-Stokes channels are allowed with available optical modes. In (b) the Stokes channel is strongly inhibited with no optical modes accessible at energies lower than that of the BL. The expected Brillouin spectra resulting from these available resonances are schematized at the top of (a) and (b). (c) Experimental intensity of the S and AS signals as a function of BL power, obtained for the resonance conditions depicted in (a) and (b), respectively, and a TL power of 10 mW (DOR condition in Fig. 2). The dashed straight line is a linear fit based on the low-power data. Shaded regions indicate the experimental uncertainty (see the SM for details [27]). The red and blue curves are guides to the eye. (d) Effective mode temperature (or, equivalently, mode occupation) for the slow SL vibrational mode deduced from the AS intensities in (c). The yellow dashed curve is a fit with a dependence of the form $n \propto 1/(1+C)$.

Consequently, the competing Stokes processes are strongly inhibited [12,19,24]. For the Stokes geometry, this is not the case: optical modes present at energies higher than that of the BL contribute through anti-Stokes channels to balance the phonon generation and thus to limit the possibility to access a self-oscillation threshold with the Gaussian photon potential used.

Optomechanical coupling and cooperativity. The main optomechanical coupling mechanism in SL-embedded semiconductor microcavities close to excitonic resonance is photoelastic (an electrostrictive optical force) [37,38]. The single-photon photoelastic coupling rate g_0 can be calculated from the overlap integral of the normalized incident and scattered optical [$\mathcal{E}(z)$] and strain [$\partial_z u_{\rm m}(z)$] fields as [31]

$$g_0 = \mathcal{K}\frac{1}{\sqrt{D_{\rm i}\,D_{\rm s}}}\int_L \epsilon_{\rm r}^2(z)\,p_{12}(z)\partial_z u_{\rm m}(z)\,\mathcal{E}^*_{\omega_{\rm s}}(z)\,\mathcal{E}_{\omega_{\rm i}}(z)\,dz, \quad (1)$$

where $\mathcal{K} = \frac{1}{\epsilon_{\rm r}^{\rm eff} L_{\rm opt}^{\rm eff}}\sqrt{\frac{\hbar\,\omega_{\rm s}\,\omega_{\rm i}}{2\,\pi\,\Omega_{\rm m}}}$. Here $\epsilon_{\rm r}^{\rm eff} = d_{\rm T}^{-1}\sum_j \epsilon_j\,d_j$, $d_{\rm T}$ is the total structure's thickness, and d_j is the width of each individual layer of the heterostructure. $L_{\rm opt}^{\rm eff}$ is the spacer thickness plus the contribution of the exponential penetration of the field into the distributed bragg reflectors (DBRs). L is the sample thickness. $\epsilon_{\rm r}$ is the media relative permittivity. p_{12} is the material-dependent photoelastic constant, resonant in the GaAs quantum wells. And $\omega_{\rm i}$ ($\omega_{\rm s}$) and $D_{\rm i}$ ($D_{\rm s}$) are the angular frequency and effective lateral diameter of the incoming (scattered) photon mode, respectively. This expression highlights the relevance of (i) a good overlap between light and strain fields (attained for the SL slow vibrational mode [27]), (ii) a large photoelastic coupling (existent in GaAs quantum wells [33]), and (iii) a small optical mode diameter, accomplished through the Gaussian laser-engineered optical trap. We compute $g_0/2\pi = 1.8\,$MHz for the SL slow mode at $\Omega_m = 2\pi \times 180$ GHz (see [27] for details). This is a very strong optomechanical coupling, two orders of magnitude larger than the radiation pressure contribution in these devices [39].

The strength of the interaction is quantified by the optomechanical cooperativity, $C = \frac{4g_0^2 n_{\rm cav}}{\kappa\,\Gamma_{\rm m}}$. Here, $n_{\rm cav}$ is the number of photons in the cavity, and κ and $\Gamma_{\rm m}$ are the photon and mechanical decay rates, respectively [19]. The coupled optomechanical equations for *two* optical cavity modes detuned by the frequency of the phonon lead to an optomechanically modified phonon effective lifetime $\Gamma_{\rm eff} = \Gamma_{\rm m}(1 \pm C)$ [19,31]. The minus sign corresponds to stimulation (the laser exciting in the upper energy mode), while the plus sign corresponds to cooling (excitation is done in the lower energy mode). Nonlinearities require the cooperativity C to become of the order of or larger than 1. For example, for higher mode excitation $C = 1$ ($\Gamma_{\rm eff} = 0$) defines the phonon "lasing" threshold.

The self-oscillation threshold power for the two-mode ($P_{\rm Th}^{(2)}$) configuration is related to that for the one-mode ($P_{\rm Th}^{(1)}$) configuration by $P_{\rm Th}^{(2)} = P_{\rm Th}^{(1)}/(1 + 4\frac{\Omega_{\rm m}^2}{\kappa^2})$ [31]. For the system under consideration $\Omega_{\rm m}/2\pi \sim 180\,$GHz $> \kappa/2\pi \sim 75\,$GHz. That is, $P_{\rm Th}^{(1)} \sim 24 \times P_{\rm Th}^{(2)}$. The factor of 24 arises because one of the two photons intervening in the optomechanical process is detuned with respect to the optical cavity mode and thus a larger external laser power is required to inject the intracavity photons required to attain self-oscillation. This explains the smaller intensity of the SORs when compared to the DOR processes in Fig. 3(b). Consideration of the relative contribution of single- and double-resonant optical processes based on this factor and that of the mode lateral size dependence $1/D$ discussed above and extracted from the experimental spatial images in Fig. 1 allows us to phenomenologically model the Brillouin intensity dependence with TL power as shown by the solid line in Fig. 2(b) (details are included in [27]).

While this model describes quantitatively the relative contribution of the different resonances, evaluation of the conditions needed for cooling or self-oscillation requires additional considerations. In fact, there are important assumptions implicit in the equation $\Gamma_{\rm eff} = \Gamma_{\rm m}(1 \pm C)$, the most relevant being that only the two described DOR optical modes are available for the optomechanical processes, with no competing inverse channels present. As discussed above, this is a reasonable description of the anti-Stokes geometry in Fig. 3(b) but not of the Stokes one in Fig. 3(a). We thus concentrate next only on the cooling geometry. With g_0 obtained from Eq. (1), using $\kappa = 2\pi \times 75$ GHz, $\Gamma_m = 2\pi \times 160$ MHz, and the intracavity photon number $n_{\rm cav} = P/(\hbar\omega\kappa) \approx 2 \times 10^6$ for a BL power of $P_{\rm BL} \sim 10$ mW as used in the cooling experiment of Fig. 3(d), we obtain $C \sim 2$. Thus, a reduction of the phonon occupation by a factor of $\sim$3 is expected, as observed in the experiment ($\Gamma_{\rm eff} \sim 3\,\Gamma_{\rm m}$). In fact, a fit to the cooling data assuming a dependence of the form $n \propto 1/(1 + C)$ [shown by the dashed yellow curve in Fig. 3(d)] yields the experimental determination $g_0^{\rm exp}/2\pi \sim 1.83\,$MHz, notably coincident with the theoretical estimation from Eq. (1).

We have demonstrated that laser-generated 3D optical traps in a planar semiconductor microcavity lead to a strong enhancement of the optomechanical coupling. Compared to optical confinement using etched traps, the proposed scheme does not require technologically complex techniques of device microfabrication and avoids lateral edges, which are known to be limiting factors for both the photon and phonon lifetimes [30]. The laser-generated Gaussian trap allowed for optomechanical cooling of the slow $\sim$180-GHz vibrational mode of a GaAs/AlAs SL by $\sim$200 K from room temperature down to $\sim$130 K. The large magnitude and resonant character of the electrostrictive optomechanical coupling [33] and the accessed sideband-resolved regime allow us to envisage the possibility to laser cool these extremely high frequency vibrations down to the quantum regime even at room temperatures. In addition, proper design of the photon potential to quench the limiting anti-Stokes channels should allow for phonon lasing. This could be attained with the Gaussian potential demonstrated here using single outgoing resonances with smaller energy vibrations (such as the 20-GHz confined modes known to exist in these structures [30]), or, alternatively, by designing more complex potentials through structured illumination as demonstrated in the framework of polaritonics, for example, in Ref. [9]. Indeed, it is straightforward to extend the results reported here to the polariton regime, in which intrinsic lasing of the system can be exploited to boost a mechanical self-oscillation regime [40]. Our results thus open new roads in the conception of hybrid devices based on cavity quantum electrodynamical and

optomechanical phenomena based on reconfigurable laser potential landscape engineering.

Acknowledgments. We acknowledge partial financial support from the ANPCyT-FONCyT (Argentina) under Grants No. PICT2015-1063 and No. PICT-2018-03255 and from the Universidad Nacional de Cuyo (Argentina) under Grants No. C034 and No. 06/C554.

[1] C. Schneider, K. Winkler, M. D. Fraser, M. Kamp, Y. Yamamoto, E. A. Ostrovskaya, and S. Höfling, Exciton-polariton trapping and potential landscape engineering, Rep. Prog. Phys. **80**, 016503 (2016).

[2] E. Wertz, L. Ferrier, D. D. Solnyshkov, R. Johne, D. Sanvitto, A. Lemaître, I. Sagnes, R. Grousson, A. V. Kavokin, P. Senellart, G. Malpuech, and J. Bloch, Spontaneous formation and optical manipulation of extended polariton condensates, Nat. Phys. **6**, 860 (2010).

[3] G. Tosi, G. Christmann, N. G. Berloff, P. Tsotsis, T. Gao, Z. Hatzopoulos, P. G. Savvidis, and J. J. Baumberg, Sculpting oscillators with light within a nonlinear quantum fluid, Nat. Phys. **8**, 190 (2012).

[4] M. Abbarchi, A. Amo, V. G. Sala, D. D. Solnyshkov, H. Flayac, L. Ferrier, I. Sagnes, E. Galopin, A. Lemaître, G. Malpuech, and J. Bloch, Macroscopic quantum self-trapping and Josephson oscillations of exciton polaritons, Nat. Phys. **9**, 275 (2013).

[5] A. Dreismann, P. Cristofolini, R. Balili, G. Christmann, F. Pinsker, N. G. Berloff, Z. Hatzopoulos, P. G. Savvidis, and J. J. Baumberg, Coupled counterrotating polariton condensates in optically defined annular potentials, Proc. Natl. Acad. Sci. USA **111**, 8770 (2014).

[6] M. Pieczarka, M. Boozarjmehr, E. Estrecho, Y. Yoon, M. Steger, K. West, L. N. Pfeiffer, K. A. Nelson, D. W. Snoke, A. G. Truscott, and E. A. Ostrovskaya, Effect of optically induced potential on the energy of trapped exciton polaritons below the condensation threshold, Phys. Rev. B **100**, 085301 (2019).

[7] S. Anguiano, A. A. Reynoso, A. E. Bruchhausen, A. Lemaître, J. Bloch, and A. Fainstein, Three-dimensional trapping of light with light in semiconductor planar microcavities, Phys. Rev. B **99**, 195308 (2019).

[8] M. Boozarjmehr, M. Steger, K. West, L. N. Pfeiffer, D. W. Snoke, A. G. Truscott, E. A. Ostrovskaya, and M. Pieczarka, Spatial distribution of an optically induced excitonic reservoir below exciton-polariton condensation threshold, arXiv:1912.07765.

[9] S. Alyatkin, J. D. Töpfer, A. Askitopoulos, H. Sigurdsson, and P. G. Lagoudakis, Optical Control of Couplings in Polariton Condensate Lattices, Phys. Rev. Lett. **124**, 207402 (2020).

[10] V. Letokhov, V. Minogin, and B. Pavlik, Cooling and capture of atoms and molecules by a resonant light field, Zh. Eksp. Teor. Fiz. **72**, 1328 (1977).

[11] D. J. Wineland and W. M. Itano, Laser cooling of atoms, Phys. Rev. A **20**, 1521 (1979).

[12] C. Monroe, D. M. Meekhof, B. E. King, S. R. Jefferts, W. M. Itano, D. J. Wineland, and P. Gould, Resolved-Sideband Raman Cooling of a Bound Atom to the 3D Zero-Point Energy, Phys. Rev. Lett. **75**, 4011 (1995).

[13] R. Chang, A. L. Hoendervanger, Q. Bouton, Y. Fang, T. Klafka, K. Audo, A. Aspect, C. I. Westbrook, and D. Clément, Three-dimensional laser cooling at the doppler limit, Phys. Rev. A **90**, 063407 (2014).

[14] R. M. Pettit, W. Ge, P. Kumar, D. R. Luntz-Martin, J. T. Schultz, L. P. Neukirch, M. Bhattacharya, and A. N. Vamivakas, An optical tweezer phonon laser, Nat. Photonics **13**, 402 (2019).

[15] D. Windey, C. Gonzalez-Ballestero, P. Maurer, L. Novotny, O. Romero-Isart, and R. Reimann, Cavity-Based 3D Cooling of a Levitated Nanoparticle via Coherent Scattering, Phys. Rev. Lett. **122**, 123601 (2019).

[16] U. Delić, M. Reisenbauer, K. Dare, D. Grass, V. Vuletić, N. Kiesel, and M. Aspelmeyer, Cooling of a levitated nanoparticle to the motional quantum ground state, Science **367**, 892 (2020).

[17] O. Arcizet, P.-F. Cohadon, T. Briant, M. Pinard, and A. Heidmann, Radiation-pressure cooling and optomechanical instability of a micromirror, Nature (London) **444**, 71 (2006).

[18] T. J. Kippenberg and K. J. Vahala, Cavity optomechanics: Back-action at the mesoscale, Science **321**, 1172 (2008).

[19] M. Aspelmeyer, T. J. Kippenberg, and F. Marquardt, Cavity optomechanics, Rev. Mod. Phys. **86**, 1391 (2014).

[20] A. D. O'Connell, M. Hofheinz, M. Ansmann, R. C. Bialczak, M. Lenander, E. Lucero, M. Neeley, D. Sank, H. Wang, M. Weides, J. Wenner, J. M. Martinis, and A. N. Cleland, Quantum ground state and single-phonon control of a mechanical resonator, Nature (London) **464**, 697 (2010).

[21] J. D. Teufel, T. Donner, D. Li, J. W. Harlow, M. S. Allman, K. Cicak, A. J. Sirois, J. D. Whittaker, K. W. Lehnert, and R. W. Simmonds, Sideband cooling of micromechanical motion to the quantum ground state, Nature (London) **475**, 359 (2011).

[22] J. Chan, T. P. M. Alegre, A. H. Safavi-Naeini, J. T. Hill, A. Krause, S. Gröblacher, M. Aspelmeyer, and O. Painter, Laser cooling of a nanomechanical oscillator into its quantum ground state, Nature (London) **478**, 89 (2011).

[23] E. Verhagen, S. Deléglise, S. Weis, A. Schliesser, and T. J. Kippenberg, Quantum-coherent coupling of a mechanical oscillator to an optical cavity mode, Nature (London) **482**, 63 (2012).

[24] L. Qiu, I. Shomroni, P. Seidler, and T. J. Kippenberg, Laser Cooling of a Nanomechanical Oscillator to its Zero-Point Energy, Phys. Rev. Lett. **124**, 173601 (2020).

[25] T. J. Kippenberg, H. Rokhsari, T. Carmon, A. Scherer, and K. J. Vahala, Analysis of Radiation-Pressure Induced Mechanical Oscillation of an Optical Microcavity, Phys. Rev. Lett. **95**, 033901 (2005).

[26] I. S. Grudinin, H. Lee, O. Painter, and K. J. Vahala, Phonon Laser Action in a Tunable Two-Level System, Phys. Rev. Lett. **104**, 083901 (2010).

[27] See Supplemental Material at http://link.aps.org/supplemental/10.1103/PhysRevB.103.L081301, which includes Refs. [41–53], for further details on the sample and performed experiments, some additional results, and the different aspects considered for the theoretical modeling.

[28] M. Trigo, T. A. Eckhause, M. Reason, R. S. Goldman, and R. Merlin, Observation of Surface-Avoiding Waves: A New Class of Extended States in Periodic Media, Phys. Rev. Lett. **97**, 124301 (2006).

[29] V. Villafañe, P. Soubelet, A. E. Bruchhausen, N. D. Lanzillotti-Kimura, B. Jusserand, A. Lemaître, and A. Fainstein, Slow light and slow acoustic phonons in optophononic resonators, Phys. Rev. B **94**, 205308 (2016).

[30] S. Anguiano, P. Sesin, A. E. Bruchhausen, F. R. Lamberti, I. Favero, M. Esmann, I. Sagnes, A. Lemaître, N. D. Lanzillotti-Kimura, P. Senellart, and A. Fainstein, Scaling rules in optomechanical semiconductor micropillars, Phys. Rev. A **98**, 063810 ((2018).

[31] P. Kharel, G. I. Harris, E. A. Kittlaus, W. H. Renninger, N. T. Otterstrom, J. G. E. Harris, and P. T. Rakich, High-frequency cavity optomechanics using bulk acoustic phonons, Sci. Adv. **5**, eaav0582 (2019).

[32] N. T. Otterstrom, R. O. Behunin, E. A. Kittlaus, and P. T. Rakich, Optomechanical Cooling in a Continuous System, Phys. Rev. X **8**, 041034 (2018).

[33] B. Jusserand, A. N. Poddubny, A. V. Poshakinskiy, A. Fainstein, and A. Lemaître, Polariton Resonances for Ultrastrong Coupling Cavity Optomechanics in GaAs/AlAs Multiple Quantum Wells, Phys. Rev. Lett. **115**, 267402 (2015).

[34] K. Kneipp, Y. Wang, H. Kneipp, I. Itzkan, R. R. Dasari, and M. S. Feld, Population Pumping of Excited Vibrational States by Spontaneous Surface-Enhanced Raman Scattering, Phys. Rev. Lett. **76**, 2444 (1996).

[35] R. C. Maher, P. G. Etchegoin, E. C. L. Ru, and L. F. Cohen, A conclusive demonstration of vibrational pumping under surface enhanced raman scattering conditions, J. Phys. Chem. B **110**, 11757 (2006).

[36] A. B. Shkarin, A. D. Kashkanova, C. D. Brown, S. Garcia, K. Ott, J. Reichel, and J. G. E. Harris, Quantum Optomechanics in a Liquid, Phys. Rev. Lett. **122**, 153601 (2019).

[37] C. Baker, W. Hease, D.-T. Nguyen, A. Andronico, S. Ducci, G. Leo, and I. Favero, Photoelastic coupling in gallium arsenide optomechanical disk resonators, Opt. Express **22**, 14072 (2014).

[38] V. Villafañe, S. Anguiano, A. E. Bruchhausen, G. Rozas, J. Bloch, C. G. Carbonell, A. Lemaître, and A. Fainstein, Quantum well photoelastic comb for ultra-high frequency cavity optomechanics, Quantum Sci. Technol. **4**, 014011 (2018).

[39] V. Villafañe, P. Sesin, P. Soubelet, S. Anguiano, A. E. Bruchhausen, G. Rozas, C. G. Carbonell, A. Lemaître, and A. Fainstein, Optoelectronic forces with quantum wells for cavity optomechanics in GaAs/AlAs semiconductor microcavities, Phys. Rev. B **97**, 195306 (2018).

[40] D. L. Chafatinos, A. S. Kuznetsov, S. Anguiano, A. E. Bruchhausen, A. A. Reynoso, K. Biermann, P. V. Santos, and A. Fainstein, Polariton-driven phonon laser, Nat. Commun. **11**, 4552 (2020).

[41] J. Talghader and J. S. Smith, Thermal dependence of the refractive index of GaAs and AlAs measured using semiconductor multilayer optical cavities, Appl. Phys. Lett. **66**, 335 (1995).

[42] G. Rozas, A. E. Bruchhausen, A. Fainstein, B. Jusserand, and A. Lemaître, Polariton path to fully resonant dispersive coupling in optomechanical resonators, Phys. Rev. B **90**, 201302(R) (2014).

[43] C. Weisbuch, M. Nishioka, A. Ishikawa, and Y. Arakawa, Observation of the Coupled Exciton-Photon Mode Splitting in a Semiconductor Quantum Microcavity, Phys. Rev. Lett. **69**, 3314 (1992).

[44] A. Fainstein, B. Jusserand, and V. Thierry-Mieg, Raman Scattering Enhancement by Optical Confinement in a Semiconductor Planar Microcavity, Phys. Rev. Lett. **75**, 3764 (1995).

[45] M. Trigo, A. Fainstein, B. Jusserand, and V. Thierry-Mieg, Finite-size effects on acoustic phonons in GaAs/AlAs superlattices, Phys. Rev. B **66**, 125311 (2002).

[46] S. M. Rytov, Acoustical properties of a thinly laminated medium, Akust. Zh. **2**, 71 (1956).

[47] B. Jusserand and M. Cardona, Raman Spectroscopy of vibrations in superlattices, in *Light Scattering in Solids V: Superlattices and Other Microstructures*, edited by M. Cardona and G. Güntherodt (Springer, Berlin, 1989), pp. 49–152.

[48] A. Fainstein, N. D. Lanzillotti-Kimura, B. Jusserand, and B. Perrin, Strong Optical-Mechanical Coupling in a Vertical GaAs/AlAs Microcavity for Subterahertz Phonons and Near-Infrared Light, Phys. Rev. Lett. **110**, 037403 (2013).

[49] A. Fainstein and B. Jusserand, Raman scattering in resonant cavities, in *Light Scattering in Solids IX: Novel Materials and Techniques*, edited by M. Cardona and R. Merlin (Springer, Berlin, 2007), pp. 17–110.

[50] J. He, B. Djafari-Rouhani, and J. Sapriel, Theory of light scattering by longitudinal-acoustic phonons in superlattices, Phys. Rev. B **37**, 4086 (1988).

[51] P. T. Rakich, P. Davids, and Z. Wang, Tailoring optical forces in waveguides through radiation pressure and electrostrictive forces, Opt. Express **18**, 14439 (2010).

[52] L. D. Landau and E. M. Lifshitz, *Theory of Elasticity*, Course of Theoretical Physics Vol. 7 (Pergamon, Oxford, London, 1986).

[53] D. Babic and S. Corzine, Analytic expressions for the reflection delay, penetration depth, and absorptance of quarter-wave dielectric mirrors, IEEE J. Quantum Electron. **28**, 514 (1992).